A Novel Framework for Metric-Based Image Registration

Qian Xie[1], Sebastian Kurtek[1], Gary E. Christensen[2], Zhaohua Ding[3], Eric Klassen[4], and Anuj Srivastava[1]

[1] Department of Statistics, Florida State University
[2] Department of Electrical and Computer Engineering, University of Iowa
[3] Institute of Imaging Science, Vanderbilt University
[4] Department of Mathematics, Florida State University

Abstract. The registrations of functions and images is a widely-studied problem that has seen a variety of solutions in the recent years. Most of these solutions are based on objective functions that fail to satisfy two most basic and desired properties in registration: (1) invariance under identical warping: since the registration between two images is unchanged under identical domain warping, the cost function evaluating registrations should also remain unchanged; (2) inverse consistency: the optimal registration of image A to B should be the same as that of image B to A. We present a novel registration approach that uses the L^2 norm, between certain vector fields derived from images, as an objective function for registering images. This framework satisfies symmetry and invariance properties. We demonstrate this framework using examples from different types of images and compare performances with some recent methods.

1 Introduction

The problem of image registration is one of the most widely studied problems in medical image analysis. Given a set of observed images, the goal is to register points across the domains of these images. This problem has many names: registration, matching, correspondence, re-parameterization, warping, deformation, etc but the basic problem is essentially the same – which pixel/voxel on an image matches which pixel/voxel on the other image. Although this problem has been studied for almost two decades, there continue to be some fundamental limitations in the popular solutions that make them suboptimal, difficult to evaluate and limited in scope.

To explain this issue consider images on a domain $\mathcal{D}$ taking the form $f : \mathcal{D} \to \mathbb{R}^n$. A pairwise registration between any two images $f_1,\ f_2$ is defined as finding a mapping γ, typically a diffeomorphism from $\mathcal{D}$ to itself, such that $f_1(s)$ and $f_2(\gamma(s))$ are optimally matched to each other (under a chosen criterion) for all $s \in \mathcal{D}$. Registration problems are commonly posed as variational problems, with the most common form of an objective function being

$$\int_{\mathcal{D}} \|f_1(s) - f_2 \circ \gamma(s)\|^2 ds + \lambda \mathcal{R}(\gamma),\ \gamma \in \Gamma\ , \tag{1}$$

where $\|\cdot\|$ is the Euclidean norm, $\mathcal{R}$ is a regularization penalty on γ commonly involving its first or second derivatives, Γ is a set of diffeomorphisms, and λ is a positive constant. Several variations of this objective function have also been used, where the first term

B.M. Dawant et al. (Eds.): WBIR 2012, LNCS 7359, pp. 276–285, 2012.

is replaced by mutual information [12], minimum description length [5], etc., and/or the second term is replaced by the length of a geodesic in the warping space (as in the LDDMM approach [3]). Another idea is to impose regularization externally using a Gaussian smoothing (diffeomorphic demons [11]) of images. Some methods optimize the objective function over a proper subset $\Gamma_0 \subset \Gamma$ (e.g. the set of volume-preserving diffeos), some on Γ, and some on larger group Γ_b that contains Γ (e.g. the one including non-diffeomorphic mappings also).

Although the numerical techniques for optimization in Eqn. 1 have become quite mature over the last ten years, these objective functions themselves have several fundamental shortcomings. We start with an important question: What should be the properties of an objective function for use in registering images? The answer to this question is difficult since we may desire different results in different contexts. In fact, one can argue that we may never have a "perfect" objective function that matches human intuition and vision. Still there is a basic set of properties that seems essential in a registration framework; some of them have been discussed previously in [4,9] and others. In the following let $L(f_1, f_2 \circ \gamma)$ denote the objective function for matching f_1 and f_2 by optimizing over γ (here γ is assumed to be applied to f_2). The most important property that we need in L is **invariance to identical warping**, defined as follows. For any $f_1, f_2 \in \mathcal{F}$, and $\gamma \in \Gamma$, this invariance implies that $L(f_1, f_2) = L(f_1 \circ \gamma, f_2 \circ \gamma)$. In case L is a proper metric, then this property is nothing but action of Γ on $\mathcal{F}$, where the action is given by $(f, \gamma) \to f \circ \gamma$, by isometries. Also, assuming that Γ is a group, this property implies that $L(f_1, f_2 \circ \gamma) = L(f_1 \circ \gamma^{-1}, f_2)$. Note that some papers that do not use the full group Γ but some finite-dimensional subset (e.g. spline-based warping functions) will not satisfy this property.

Why is this property important? Consider the two functions f_1 and f_2 shown in the left panel of Fig. 1. Even though the two functions are different, their peaks and valleys are nicely aligned. The middle panel shows an example of warping function γ and the right panel shows the warped versions $f_1 \circ \gamma$ and $f_2 \circ \gamma$. It is interesting to note that the peaks and valleys in the warped functions are still aligned. Furthermore, the full correspondence between the two functions is unchanged despite the warping. In fact, one can show that an identical warping of any two functions keeps their registration unchanged and, hence, any good objective function must have this invariance to identical warping.

There is another important property that is termed **inverse consistency** ([4,2]). This property implies that the optimal registration between two functions remains the same even if they are treated in the reverse order. That is, if $\gamma^* \in \arg\min_{\gamma \in \Gamma} L(f_1, f_2 \circ \gamma)$, then $\gamma^{*-1} \in \arg\min_{\gamma \in \Gamma} L(f_2, f_1 \circ \gamma)$. It can be shown that if we have invariance to identical warping and an additional symmetry condition ($L(f_1, f_2) = L(f_2, f_1)$), then we have inverse consistency. The symmetry condition is usually satisfied by most objective functions but the invariance condition is the one that many of them fail to meet. Without the invariance to identical warping, we will not have inverse consistency in general. So, once again that the property turns out to be paramount in registration.

We note that many of the popular objective functions ([10,12,5,11,3,9]) do not satisfy these two basic properties.

There is an additional property of interest. A majority of post-matching analyses compare registered images, and apply statistical techniques such as PCA for modeling and analysis. The question is: What should be the metric for this post-registration

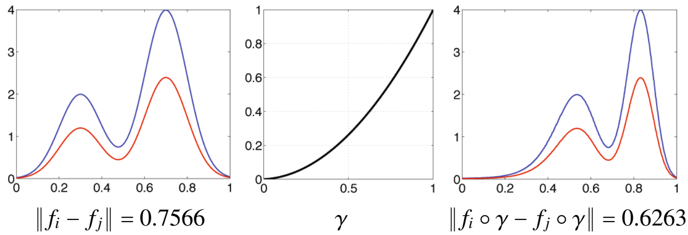

Fig. 1. An identical deformation of domains preserves the registration of functions

analyses? In many current systems, one performs registration using an objective function and then chooses a separate metric to perform analysis. Ideally, one would like a framework so that it can *align, compare, average, and model* multiple images in a **unified** framework that leads to efficient algorithms and consistent estimators. The objective function presented in this paper not only satisfies the invariance and the inverse consistency properties listed above but also forms an extrinsic metric on the quotient space for image comparison. Therefore, we have called our framework a metric-based method for registration and comparison of images.

2 Proposed Framework

In this section we lay out the framework for joint image registration and comparison under an objective function which induces an extrinsic distance. This method applies to mathematical objects whose range space has dimension at least as much as that of their domain, for $f : \mathcal{D} \to \mathbb{R}^n$, where $n \geq m, m = \dim(\mathcal{D})$. In case of 2D images, this means that pixels have at least two coordinates which is the case for colored images, or multimodal images. To register gray-scale images, we have a way to get away from this constraint, which will be discussed in Chap. 4.

Let $\mathcal{F} = \{f : \mathcal{D} \to \mathbb{R}^n \,|\, f \in C^\infty(\mathcal{D}), \|f\| = 1\}$ and $\Gamma = \{\gamma : \mathcal{D} \to \mathcal{D} \,|\, \gamma \in \mathrm{Diff}(\mathcal{D})\}$, where $\|\cdot\|$ denotes the standard $\mathbb{L}^2$ norm and Diff($\mathcal{D}$) is the diffeomorphism group on $\mathcal{D}$. The action of Γ on $\mathcal{F}$ is defined as follows.

Definition 1. *For an $f \in \mathcal{F}$, define the right action $\mathcal{F} \times \Gamma \to \mathcal{F}$ by $(f, \gamma) = f \circ \gamma$.*

Note that for any two $f_1, f_2 \in \mathcal{F}$, and a $\gamma \in \Gamma$, we usually have $\|f_1 - f_2\| \neq \|f_1 \circ \gamma - f_2 \circ \gamma\|$ and invariance consition is not satisfied. Thus, we do not work with the images directly. Instead, we will use a novel mathematical representation of images, called a q-map, that has been motivated by recent work in shape analysis of surfaces [7]. Here we adapt it for analyzing images.

Definition 2. *For an $f \in \mathcal{F}$, define a mapping $Q : \mathcal{F} \to \mathbb{L}^2$ such that $Q(f)(s) = \sqrt{a(s)} f(s), \forall s \in \mathcal{D}$ where $a(s)$ is the multiplication factor of f at s given by $|J_f(s)|_{\text{area}}$. For any $n \times m$ matrix A $(n \geq m)$, $|A|_{\text{area}}$ is defined as $|A|_{\text{area}} = \sqrt{\sum_{B: B \text{ is } m \times m \text{ submatrix of } A} |B|^2}$ and where $|B|$ denotes determinant of B.*

For any $f \in \mathcal{F}$, we will refer to $q = Q(f)$ as its q-map. Assuming the original set of images to be smooth, the set of all q-maps is a subset of $\mathbb{L}^2$. The corresponding action of Γ on $\mathbb{L}^2$ is given as follows.

Definition 3. *Define the right action* $\mathbb{L}^2 \times \Gamma \to \mathbb{L}^2$ *by* $(q,\gamma) = \sqrt{J_\gamma}(q \circ \gamma)$*, where* J_γ *denotes the Jacobian of* γ*.*

Note that, for an image f, $Q(f \circ \gamma) = (Q(f),\gamma)$. We define $[q] = \{(q,\gamma)|\gamma \in \Gamma\}$ to be the set (or an orbit) of all warpings of a q-map. Since all elements of $[q]$ can be obtained using warpings of the same image (and then forming the q-map), we deem them equivalent from the perspective of registration. One would like a registration cost function that equals zero when evaluated on any two elements of an orbit. Let $\mathbb{L}^2/\Gamma$ be the (quotient) set of all such orbits. The most important property of this mathematical representation is the following.

Proposition 1. *The re-parametrization group* Γ *acts on* $\mathbb{L}^2$ *by isometries under the* $\mathbb{L}^2$ *norm, i.e.* $\forall q_1, q_2 \in \mathbb{L}^2, \forall \gamma \in \Gamma, \|(q_1,\gamma) - (q_2,\gamma)\| = \|q_1 - q_2\|$.

Upon a close inspection, this proposition is exactly the same as the property of invariance to identical warping in Sect. 1. In view of this isometry, the $\mathbb{L}^2$ norm between the q-maps is a proper measure of the registration between any two images since it remains the same if the registration is unchanged. This leads to a quantity that will serve as both the registration objective function and an extrinsic distance between registered images.

Definition 4. *Define an objective function between any two images* f_1 *and* f_2*, represented by their q-maps* q_1 *and* q_2*, as* $L(f_1, f_2; \gamma) \equiv \|q_1 - (q_2,\gamma)\|$.

The registration is then solved by minimizing the objective function:

$$\gamma^* = \arg\inf_{\gamma\in\Gamma} L(f_1, f_2; \gamma) \ . \tag{2}$$

The objective function L introduced as above satisfies the properties of invariance to identical warping and inverse consistency. Therefore, we are able to compare images with the value of objective function at the optimal γ, which gives a solution to registering two images. We point out that there are some unresolved mathematical issues concerning to existence of a unique global solution for γ^*, especially its existence inside Γ rather than being on its boundary. We leave this for a future discussion and focus on a numerical approach that estimates γ^*.

3 Implementation

3.1 Gradient Method for Optimization Over Γ

The optimization problem over Γ stated in Eqn. 2 forms the crux of our registration framework and we will use a gradient descent method to solve it. Since Γ is a group, we use the gradient to solve for the incremental warping γ, on top of the previous cumulative warping γ_0, as follows. (In this way the required gradient is an element of $T_{\gamma_{id}}(\Gamma)$ and one needs to understand only that space.) We define a cost function with respect to γ as $E[\gamma] = \|q_1 - \phi(\gamma)\|^2$, where $\tilde{q}_2 = (q_2, \gamma_0)$ and $\phi : \Gamma \mapsto [q_2]$ is defined to be $\phi(\gamma) = (\tilde{q}_2, \gamma)$. Given a unit vector $b \in T_{\gamma_{id}}(\Gamma)$, the directional derivative of E at γ_{id} in the direction of b is $\langle q_1 - \phi(\gamma_{id}), \phi_*(b)\rangle\, b$, where ϕ_* is the differential of ϕ at γ_{id}. It has an explicit form which is the same as that derived for parameterized surfaces in [7]. In order to compute the gradient of E and to update γ_0 we need to specify an orthonormal basis for $T_{\gamma_{id}}(\Gamma)$.

3.2 Basis on $T_{\gamma_{id}}(\Gamma)$

In this paper, we investigate registration of 2D images with domain as $\mathcal{D} = [0,1]^2$ but the framework applied to other domains as well. In this case Γ contains all boundary preserving diffeomorphisms on $[0,1]^2$. The tangent space of Γ at identity γ_{id} is $T_{\gamma_{id}}(\Gamma) = \{b : [0,1]^2 \to [0,1]^2 \mid \ b \textit{ is a smooth tangent vector field on } [0,1]^2\}$.

We begin by constructing an orthonormal basis for $\mathbb{L}^2([0,1],\mathbb{R})$ and then extend it to the 2D case. It is known that $\mathcal{B}^{1D}_{\mathbb{L}^2} = \{\sqrt{2}\sin(2\pi nt)|n >= 1\} \cup \{\sqrt{2}\cos(2\pi nt)|n >= 1\} \cup \{1\}$ forms an orthonormal basis for $\mathbb{L}^2([0,1],\mathbb{R})$ under the $\mathbb{L}^2$ metric.

We seek an orthonormal basis for $\mathbb{L}^2([0,1],\mathbb{R})$ under the Palais metric due to some nice properties of this Riemannian metric ([8]). The Palais metric is defined as $\langle f, g\rangle = f(0)g(0) + \int_0^1 f'(t)g'(t)dt$ for $f, g \in \mathbb{L}^2([0,1],\mathbb{R})$. Under this metric an orthonormal basis of $\mathbb{L}^2([0,1],\mathbb{R})$ can be defined as $\mathcal{B}^{1D}_{Pal} = \left\{\frac{\sin(2\pi nt)}{\sqrt{2}\pi n}|n >= 1\right\} \cup \left\{\frac{\cos(2\pi nt)-1}{\sqrt{2}\pi n}|n >= 1\right\} \cup \{t\} \cup \{1\}$. It is important to note that the set $\tilde{\mathcal{B}}^{1D}_{Pal} = \left\{\frac{\sin(2\pi nt)}{\sqrt{2}\pi n}|n >= 1\right\} \cup \left\{\frac{\cos(2\pi nt)-1}{\sqrt{2}\pi n}|n >= 1\right\}$ provides an orthonormal basis of functions that vanish at $t \in \{0,1\}$. The subspace of functions that vanish at $t \in \{0,1\}$ has codimension two (due to the two imposed conditions). This means that in order to define a full orthonormal basis of $\mathbb{L}^2([0,1],\mathbb{R})$, we must add two additional elements that give linearly independent pairs of values at $t \in \{0,1\}$. We will refer to the additional elements as $\mathring{\mathcal{B}}^{1D}_{Pal}$.

We will use Cartesian product of $\mathring{\mathcal{B}}^{1D}_{Pal}$ (with elements $\mathring{b}$) and $\tilde{\mathcal{B}}^{1D}_{Pal}$ (with elements $\tilde{b}$) to construct an orthonormal basis for $[0,1]^2$. First, consider two parameters $u \in [0,1]$ and $v \in [0,1]$ that define the domain $[0,1]^2$. Begin by constructing an orthonormal basis for functions on $[0,1]^2$ that vanish at the boundaries using all possible products of elements of $\tilde{\mathcal{B}}^{1\text{D}}_{Pal}$: $\tilde{\mathcal{B}}^{2D}_{Pal} = \{\tilde{b}_i(u)\tilde{b}_j(v), 0\}_{i,j\geq 1} \cup \{0, \tilde{b}_i(u)\tilde{b}_j(v)\}_{i,j\geq 1}$. In addition, we need basis elements that are tangential to the boundaries. These can be formed using the additional basis elements $\mathring{\mathcal{B}}^{1D}_{Pal}$. Define this set as: $\mathring{\mathcal{B}}^{2D}_{Pal} = \{\tilde{b}_i(u)\mathring{b}_j(v), 0\}_{i\geq 1; j=1,2} \cup \{0, \mathring{b}_i(u)\tilde{b}_j(v)\}_{i=1,2; j\geq 1}$. Then, the union $\mathcal{B}^{2D}_{Pal} = \tilde{\mathcal{B}}^{2D}_{Pal} \cup \mathring{\mathcal{B}}^{2D}_{Pal}$ provides a basis for $T_{\gamma_{id}}(\Gamma)$ under the Palais metric given by the inner product:

$$\langle\langle f, g\rangle\rangle = \langle f(0,0), g(0,0)\rangle_{\mathbb{R}^n} + \int\int \langle \nabla f(u,v), \nabla g(u,v)\rangle_{\mathbb{R}^{2n}} dudv \ .$$

4 Experimental Results

In this section, we will present some experimental results for grayscale images and multimodal images to demonstrate the use of the framework introduced in this paper. However, in case of grayscale images, with $n = 1$, our method does not apply directly since the dimension of range is less than the dimension of the domain. Instead, we apply it on gradient images g formed using $g = \nabla f : [0,1]^2 \to \mathbb{R}^2$ and $\nabla f = (f_u, f_v)$ for $(u, v) \in [0,1]^2$. Image gradients are a type of edge measure and are often used in their own right as robust spatial features for image registration. We will use the gradient field as a *feature* to establish optimal registrations and compute distances between gray-scale images. In other words, we register and compare two images by registering their gradient images. One can obtain the original image from a gradient image using PDEs [1]. (Note that this idea of using gradients to form vector-valued images will apply to volume images also, although we will restrict ourselves to 2D images for simplicity of presentation.) In order to register two images, we can use the registered gradients and get back to images ([1]). However, this approach may lead to changes in image intensities by applying diffeomorphisms. An alternative is to consider gradients as an image feature and directly use the optimal γ to register the images. This is the method applied in this paper. We will compare our method to the diffeomorphic demons method ([6]).

4.1 Synthetic Data

As a test to evaluate the framework we proposed, we first use it to register synthetic grayscale image pairs. The images f_1 and f_2 are registered twice by first taking f_1 as the template image and estimating γ_{21} that optimally deforms f_2. Similarly, f_2 is used as the template to get γ_{12}. We show the two converged energies, $\|(q_1, \gamma_{12}) - q_2\|$ and $\|q_1 - (q_2, \gamma_{21})\|$, associated with the the optimal γ_{12} and γ_{21} to verify the symmetry.

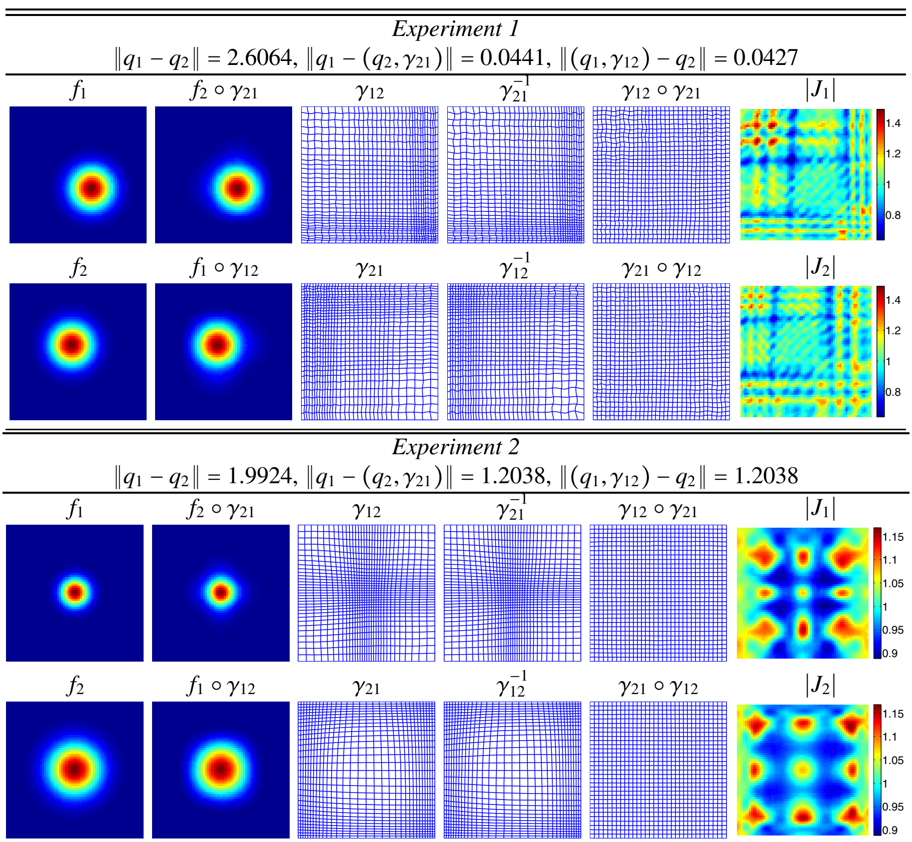

Fig. 2. Results of registration: synthetic images

The cumulative diffeomorphisms $\gamma_{21} \circ \gamma_{12}$ and $\gamma_{12} \circ \gamma_{21}$ are also used to demonstrate the symmetry of the proposed metric. In our method, γ_{12} and γ_{21} are expected to be inverses of each other.

The results for registering two datasets are shown in Fig. 2. We show the original images f_1 and f_2 with the warped images $f_2 \circ \gamma_{21}$ and $f_1 \circ \gamma_{12}$, that match with f_1 and f_2, respectively. The diffeomorphisms, γ_{12} and γ_{21} learnt to register the images are also presented. By composing them in different orders, we expect the resulting diffeomorphisms to be the identity map. In order to better visualize that the composed diffeomorphisms are close to identity, their Jacobian maps are also given. If the compositions are the exact identity map, the Jacobian images should be constant images with value 1. We observe that the composed diffeomorphisms $\gamma_{21} \circ \gamma_{12}$ and $\gamma_{12} \circ \gamma_{21}$ are close to the identity map. Although there are cases when γ_{12} and γ_{21} are not exact inverses of each other, the resulting distances are still approximately symmetric. Possible explanations include errors due to numerical interpolation of grids or γ^* being a local solution instead of a global minimizer.

4.2 Image Registration

Next, we test our method on images of hand written numbers and 2D MR images of the brain. The digit image data is used to demonstrate the performance of image registration. Figure 3 shows examples of matching three images for identical and different digit(s). Each row contains the results for a single experiment. The original images to be registered are shown in columns (a) and (d). The registration results obtained using our method are presented in columns (b) and (e). Columns (c) and (f) are the corresponding warped images using the demons method. For the experiments in Fig. 3, our registration results are at least as good as those from the demons. For many of the experiemnts, our method outperforms the other.

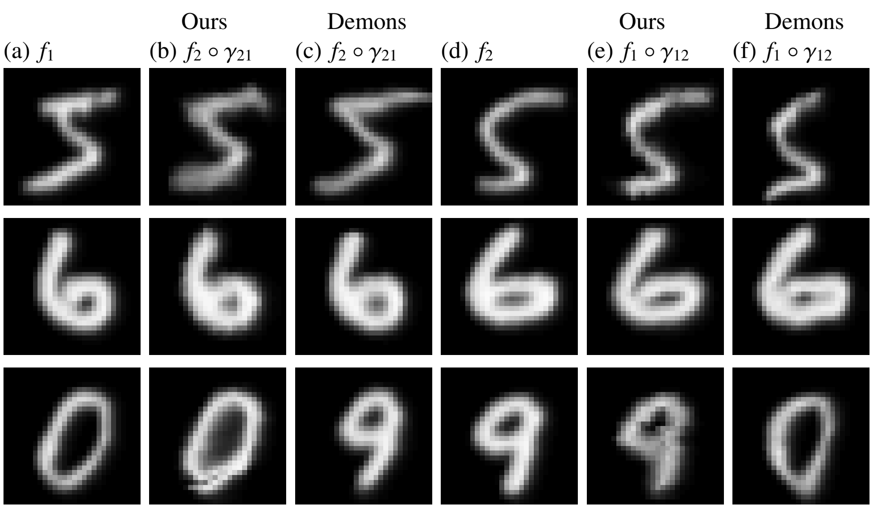

Fig. 3. Three experiments for registering digits. Each row represents an experiment

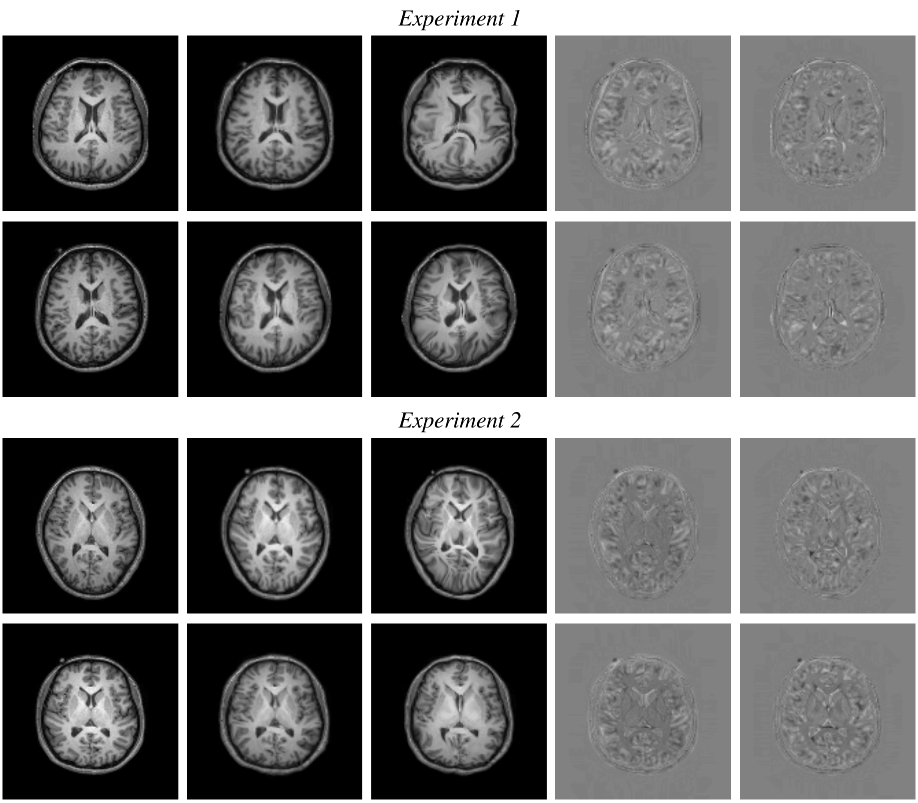

Fig. 4. Results for registering brain images. Column (a) contains two given images. The registered images from our method and diffeomorphic demons are shown in columns (b) and (c), respectively. Column (d) gives the image differences after registration using our method and column (e) contains the image differences after registration using Demons.

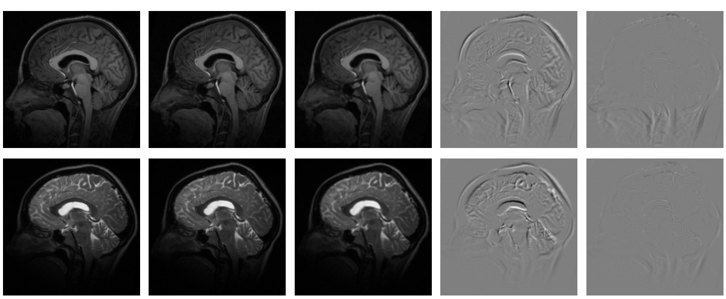

Fig. 5. Results for registering brain images from two modalities. First two columns contain given images, with the first row from T1 and the second from T2. The registered images are shown in the third column. The last two columns give the image differences before and after registration.

We also present two examples of brain MRI registration in Fig. 4. In each of the two experiments, we show the original images, our warped images, and the image differences before and after registration to illustrate our method. At the same time, the registered images from using the demons are used for comparison. For these experiments, our method provides a decent registration for the ventricular part and the boundary of the brain; most lobes remain approximately the same. The demons does not provide as good of a registration with respect to the ventricles and/or the boundaries. It also sometimes generates mistakes near the lobes.

Figure 5 shows an example of registering a pair of brain images from two modalities. Under our framework, the two modalities are registered simultaneously using the same deformation.

4.3 Image Classification

The framework introduced in this paper defined a proper distance on the space of q-maps of images. These distances can be used for pattern analysis of images, using clustering or classification. The dataset used for classification purpose contains images of digits from 0 through 9 and each digit has ten images. The distance matrices for $\mathbb{L}^2$ without warping, our method and demons are shown in Fig. 6 from (a) to (c). The $\mathbb{L}^2$ distance is automatically symmetric. We observe that the distance matrix is not symmetric for demons. Our distance matrix is approximately symmetric. The boxplots in Fig. 6 (d) are used to assess the amount of asymmetry for the distance matrices. The boxes represent the absolute values for all entries in $\left|D - D^{'}\right|/D$. These are the relative differences between diagonal entries and are supposed to be zero for a symmetric matrix. Our method provides differences closer to zero and therefore more symmetric compared to the demons method. As mentioned previously, the differences being not exactly zero may be due to computational issues such as local minima. The leave-one-out nearest-neighbor (LOO-NN) method is utilized to classify the digits based on distance matrices. The classification rates are shown in Fig. 6.

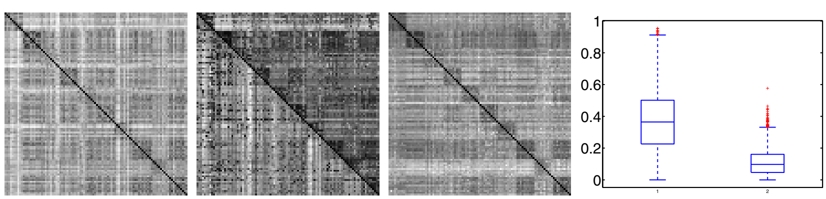

(a) $\mathbb{L}^2$, 76% (b) Demons, 79% (c) Ours, 95% (d)

Fig. 6. Classification results

5 Discussion

We proposed a unified framework to register and compare images jointly. Our distance provides a symmetric metric between image gradients and thus a good measure of registration without ambiguity. The forward and backward matching diffeomorphisms are inverses of each other when global solutions are reached. With this framework, our method gives better results for registration, comparison and classification of images compared to the demons method. Future work will involve studying mathematical properties such as injectivity of the Q map.

Acknowledgement. This research is supported in part by the Office of Naval Research under N00014-09-1-0664 and in part by the National Science Foundation under Grant DMS-0915003.

References

1. Agrawal, A., Raskar, R., Chellappa, R.: An algebraic approach to surface reconstructions from gradient fields? In: Intenational Conference on Computer Vision, ICCV (2006)
2. Avants, B., Grossman, M., Gee, J.: Symmetric diffeomorphic image registration: Evaluating automated labeling of elderly and neurodegenerative cortex and frontal lobe. Biomedical Image Registration 4057, 50–57 (2006)
3. Beg, M., Miller, M., Trouvé, A., Younes, L.: Computing large deformation metric mappings via geodesic flows of diffeomorphisms. Int. J. Comput. Vision 61, 139–157 (2005)
4. Christensen, G., Johnson, H.: Consistent image registration. IEEE Transactions on Medical Imaging 20(7), 568–582 (2001)
5. Davies, R., Twining, C., Cootes, T., Waterton, J., Taylor, C.: A minimum description length approach to statistical shape modeling. IEEE Transactions on Medical Imaging 21(5), 525–537 (2002)
6. Kroon, D., Slump, C.: MRI modalitiy transformation in demon registration. In: IEEE International Symposium on Biomedical Imaging: From Nano to Macro, ISBI 2009, pp. 963–966 (2009)
7. Kurtek, S., Klassen, E., Ding, Z., Jacobson, S., Jacobson, J., Avison, M., Srivastava, A.: Parameterization-invariant shape comparisons of anatomical surfaces. IEEE Transactions on Medical Imaging 30(3), 849–858 (2011)
8. Palais, R.: Morse theory on Hilbert manifolds. Topology 2, 299–340 (1963)
9. Tagare, H., Groisser, D., Skrinjar, O.: Symmetric non-rigid registration: A geometric theory and some numerical techniques. Journal of Mathematical Imaging and Vision 34, 61–88 (2009)
10. Taquet, M., Macq, B., Warfield, S.: A generalized correlation coefficient: application to DTI and multi-fiber DTI. In: MMBIA 2012 (2012)
11. Vercauteren, T., Pennec, X., Perchant, A., Ayache, N.: Diffeomorphic demons: Efficient non-parametric image registration. NeuroImage 45(1, supplement 1), S61–S72 (2009)
12. Viola, P., Wells III, W.M.: Alignment by maximization of mutual information. In: Proceedings of Fifth International Conference on Computer Vision, pp. 16–23 (June 1995)